Supplement of Atmos. Chem. Phys., 18, 11927–11948, 2018
https://doi.org/10.5194/acp-18-11927-2018-supplement

Atmospheric Chemistry and Physics
Open Access
EGU

Supplement of

Extremal dependence between temperature and ozone over the continental US

Pakawat Phalitnonkiat et al.

Correspondence to: Peter G. M. Hess (pgh25@cornell.edu)

Supplement

In the supplement we include results from the REEFCS1D simulations from 1992-2010 for an additional four models: the CHASER, CMAM, MOCAGE, and MRI models. The number of additional models analyzed is limited to those with sufficient output to derive the maximum daily temperature and the maximum daily 8-hour average ozone concentrations. In the CMAM and MRI simulations both ozone and temperature data are available at high temporal resolution; in the CHASER and MOCAGE simulations only high temporal resolution ozone data is available. Details on the additional model simulations is given in (see Morgenstern et al., 2017). In addition, we give additional measurement data in the supplement from the Environmental Protection Agency (EPA) Air Quality System (AQS) Data Mart for the years 1992-2010. This gives an additional 124 stations with nearly complete ozone and temperature data.

Figure S1 gives the mean rescaled maximum temperature and the 90^{th} percentile minus mean rescaled maximum temperature from the CCMI REFC1SD simulations for June, July and August (JJA) from 1992-2010 for the CNAM and MRI models. Also shown are the equivalent quantities as measured at the EPA AQS measurement sites. Figure S2 and S3 gives the same quantities but for MDA8 ozone. The equivalent quantities from for CESM1 CAM4-chem are given in Figures 2a, b and 3a, b.

Figure S4 and S5 gives the twenty-year return level minus average MDA8 ozone (ppb) for JJA from 1992-2010 for the four models: CHASER, CMAM, MOCAGE and MRI. Figure S4 gives the same metrics but for daily maximum temperature for the CMAM and MRI models. Figure S4 also gives the equivalent quantities as measured for daily maximum temperature and MDA8 ozone at the EPA AQS measurement sites. The equivalent quantities from CESM1 CAM4-chem are given in Figures 5.

Figure S6 gives the unconditional correlation between daily maximum temperature and MDA8 ozone (first column); correlations between daily maximum temperature and MDA8 ozone conditioned on maximum temperature greater than the 90th percentile (second column) and the equivalent quantities as measured for temperature and ozone at the EPA AQS measurement sites. The equivalent quantities from CESM1 CAM4-chem are given in Figure 6.

Figure S7 gives average MDA8 ozone (ppb) conditioned on daily maximum temperature greater than the 90th percentile minus average MDA ozone and φ from the CMAM and MRI REFC1SD simulations. The equivalent quantities as measured for temperature and ozone at the EPA AQS measurement sites are also given. See Figures 7 and 9 for results from the CESM1 CAM4-chem.

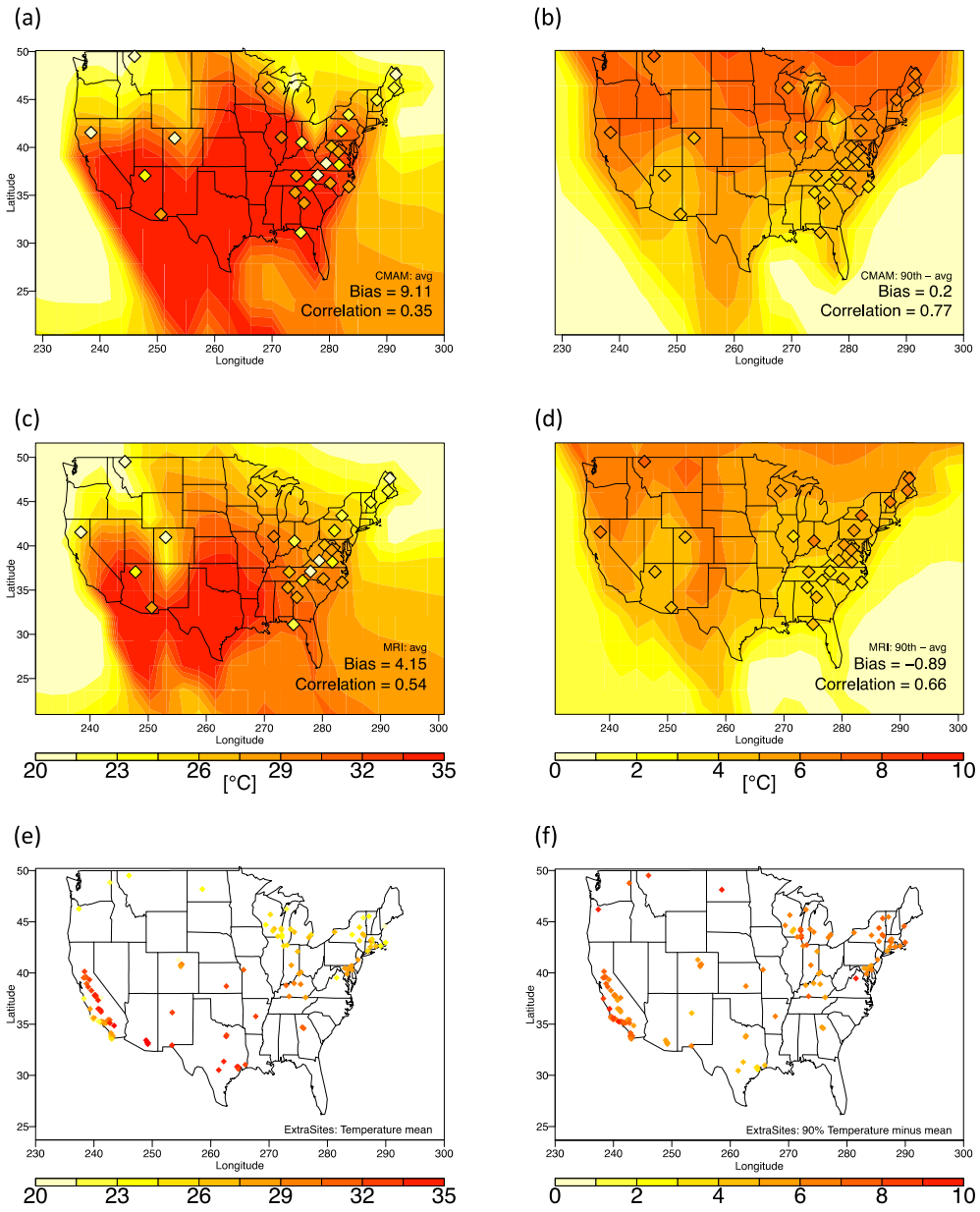

Figure S1. [Rescaled Data] Average daily maximum temperature (^{o}C) (left column) and average daily maximum temperature (^{o}C) conditioned on daily maximum temperature greater than the 90th percentile minus average maximum temperature (right column) for JJA 1992-2010. CMAM REFC1SD simulation (first row: a and b) and MRI REFC1SD simulation (second row: c and d), EPA AQS measurements (third row: e and f). CASTNET measurements of each quantity are shown as filled diamonds in the first two rows. In the first two rows we also give: the average bias as the model average minus the CASTNET average for each quantity, and the correlation as the spatial correlation between the model and the CASTNET measurements. The corresponding figure for the CESM1 CAM4-chem is given in Figure 2.

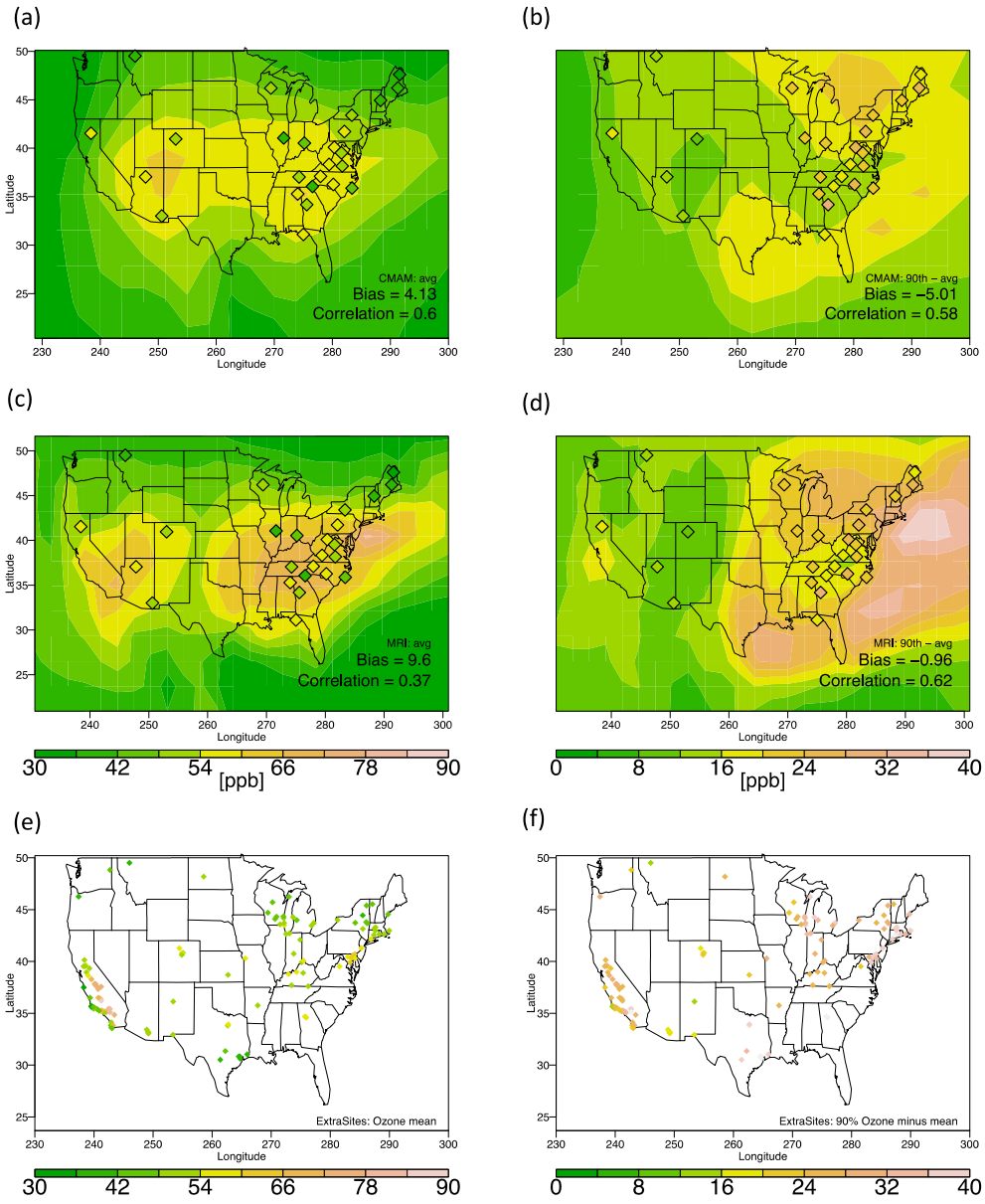

Figure S2. [Rescaled Data] Average MDA8 ozone (ppb) (left column) and average MDA8 ozone (ppb) conditioned on ozone greater than the 90th percentile minus average MDA8 ozone (right column) for JJA 1992-2010. CMAM REFC1SD simulation (first row: a and b), MRI REFC1SD simulation (second row: c and d), and EPA AQS measurements (third row: e and f). CASTNET measurements of each quantity are shown as filled diamonds in the first two rows. In the first two rows we also give: the average bias as the model average minus the CASTNET average for each quantity, and the correlation as the spatial correlation between the model and the CASTNET measurements. The corresponding figure for the CESM1 CAM4-chem is given in Figure 3.

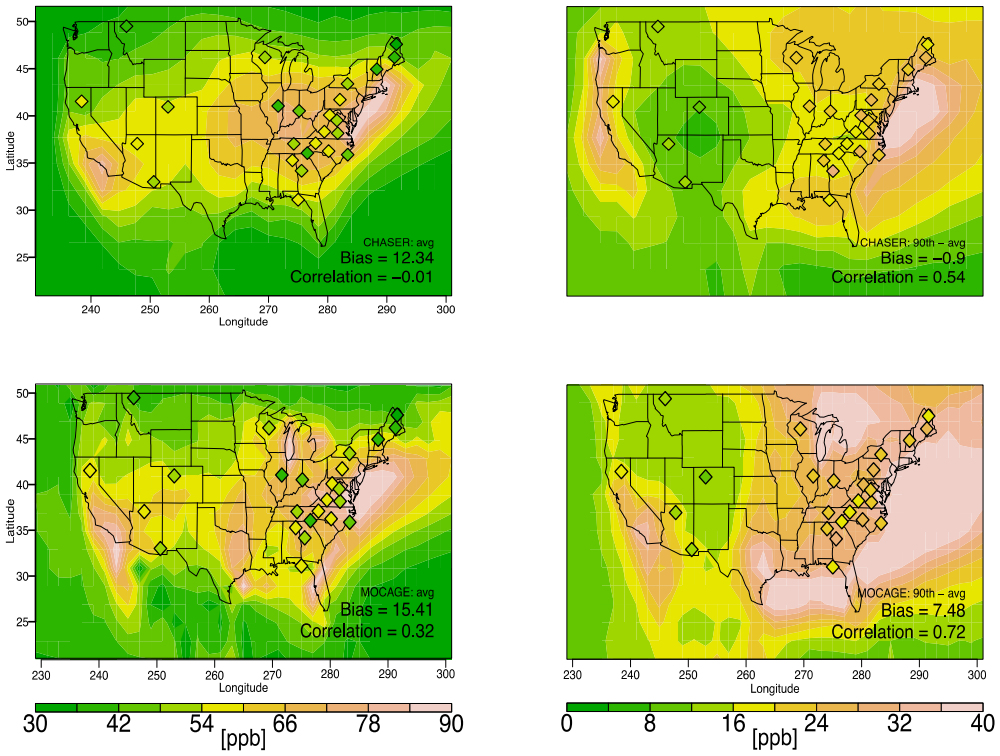

Figure S3. [Rescaled Data] Average MDA8 ozone (ppb) (left column) and average MDA8 ozone (ppb) conditioned on MDA8 ozone greater than the 90th percentile minus average MDA8 ozone (right column) for JJA 1992-2010. CHASER REFC1SD simulation (first row: a and b), and MOCAGE REFC1SD simulation (second row: c and d). CASTNET measurements of each quantity are shown as filled diamonds in the first two rows. In the first two rows we also give: the average bias as the model average minus the CASTNET average for each quantity, and the correlation as the spatial correlation between the model and the CASTNET measurements. The corresponding figure for the CESM1 CAM4-chem is given in Figure 3.

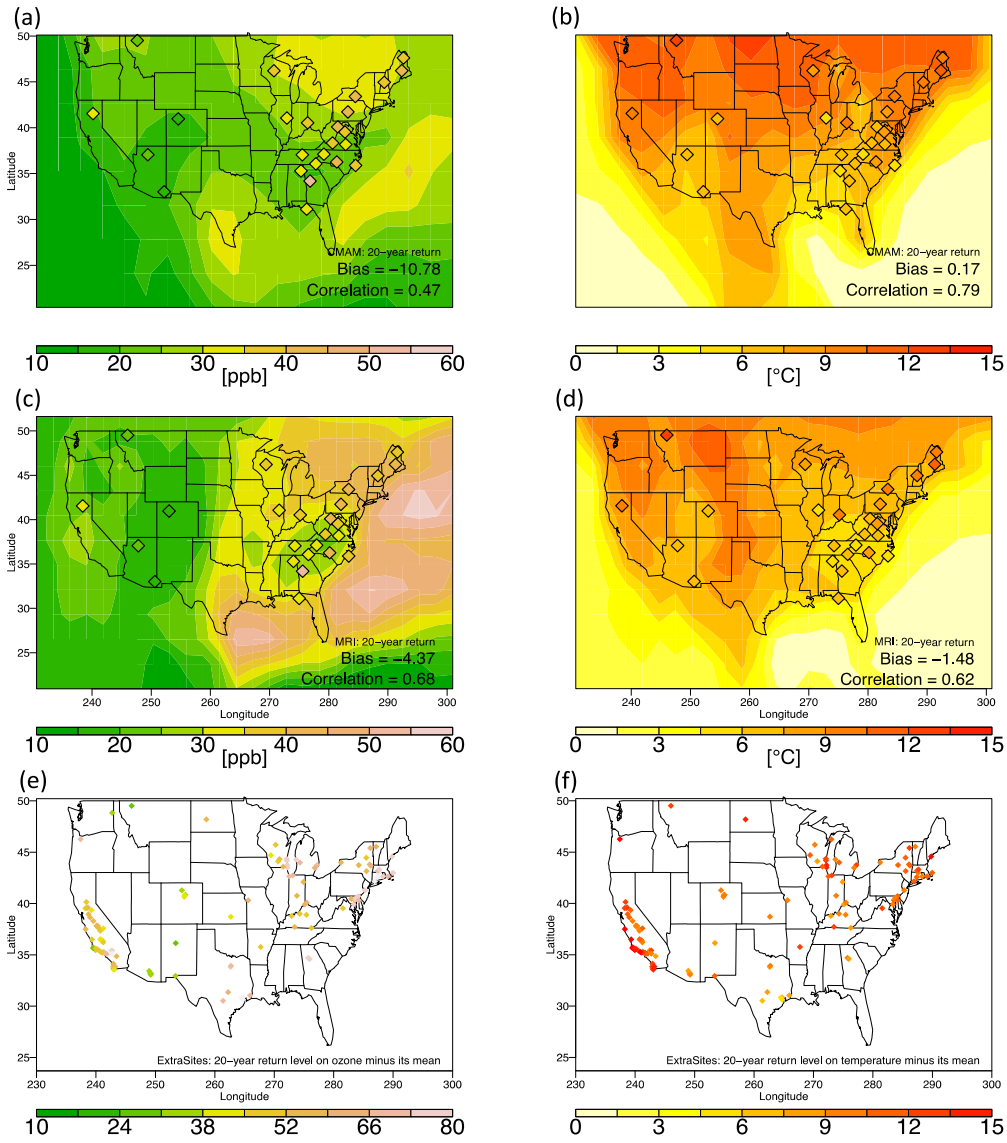

Figure S4 [Rescaled Data] Twenty-year return level minus average MDA8 ozone (ppb) (left column), and 20-year return level for daily maximum temperature minus average daily maximum temperature (right column) for JJA 1992-2010. CMAM REFC1SD simulation (first row: a and b), MRI REFC1SD simulation (second row: c and d), and EPA AQS measurements (third row: e and f). CASTNET measurements of each quantity are shown as filled diamonds in the first two rows. In the first two rows we also give: the average bias as the model average minus the CASTNET average for each quantity, and the correlation as the spatial correlation between the model and the CASTNET measurements. The corresponding figure for the CESM1 CAM4-chem is given in Figure 5.

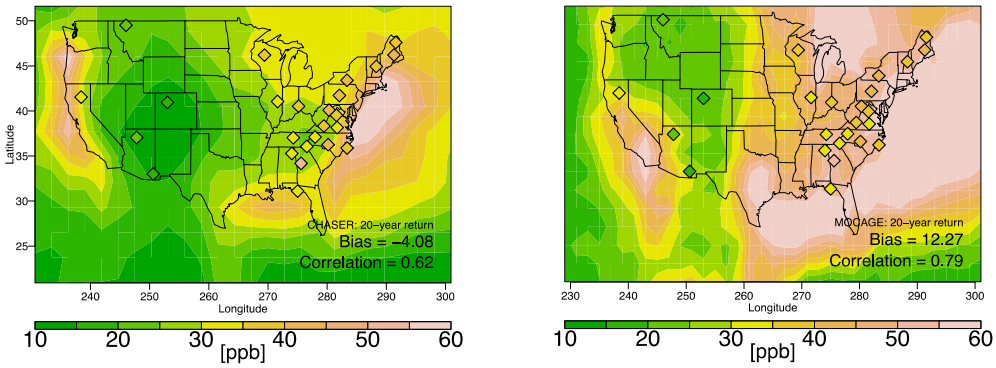

Figure S5 [Rescaled Data] Twenty-year return level minus average MDA8 ozone (ppb) (left column) for JJA 1992-2010. CHASER REFC1SD simulation (a), and MOCAGE REFC1SD simulation (b). We also give the average bias as the model average minus the CASTNET average for each quantity, and the correlation as the spatial correlation between the model and the CASTNET measurements. The corresponding figure for the CESM1 CAM4-chem is given in Figure 5.

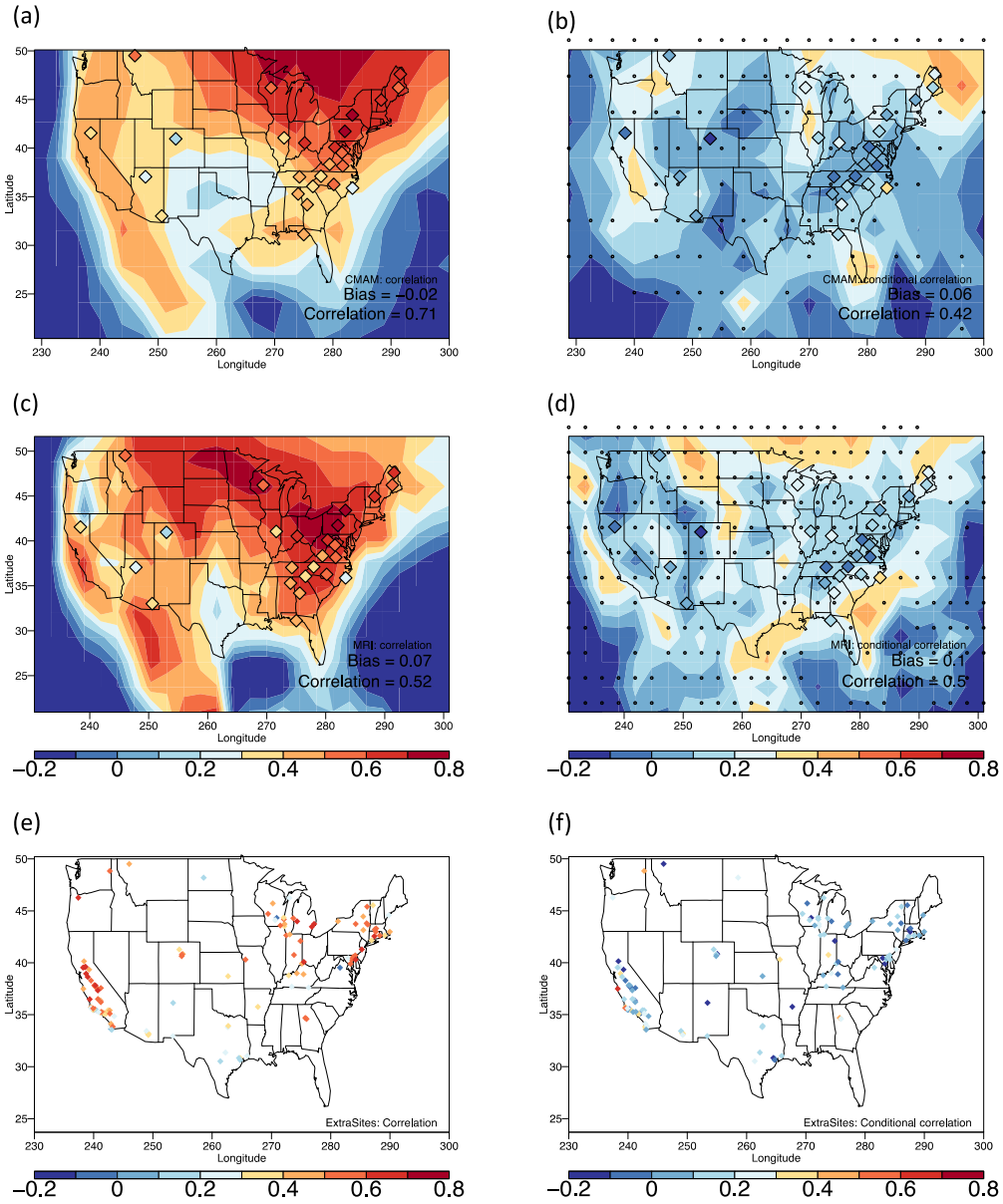

Figure S6 [Deseasonalized Data] Unconditional correlations between daily maximum temperature and MDA8 ozone (first column); correlations between daily maximum temperature and MDA8 ozone conditional on daily maximum temperature greater than the 90th percentile (second column) for JJA 1992-2010. CMAM REFC1SD simulation (first row: a and b), MRI REFC1SD simulation (second row: c and d), and EPA AQS measurements (third row: e and f). CASTNET measurements of each quantity are shown as filled diamonds in the first two rows. In the first two rows we also give: the average bias as the model average minus the CASTNET average for each quantity, and the correlation as the spatial correlation between the model and the CASTNET measurements. The corresponding figure for the CESM1 CAM4-chem is given in Figure 6.

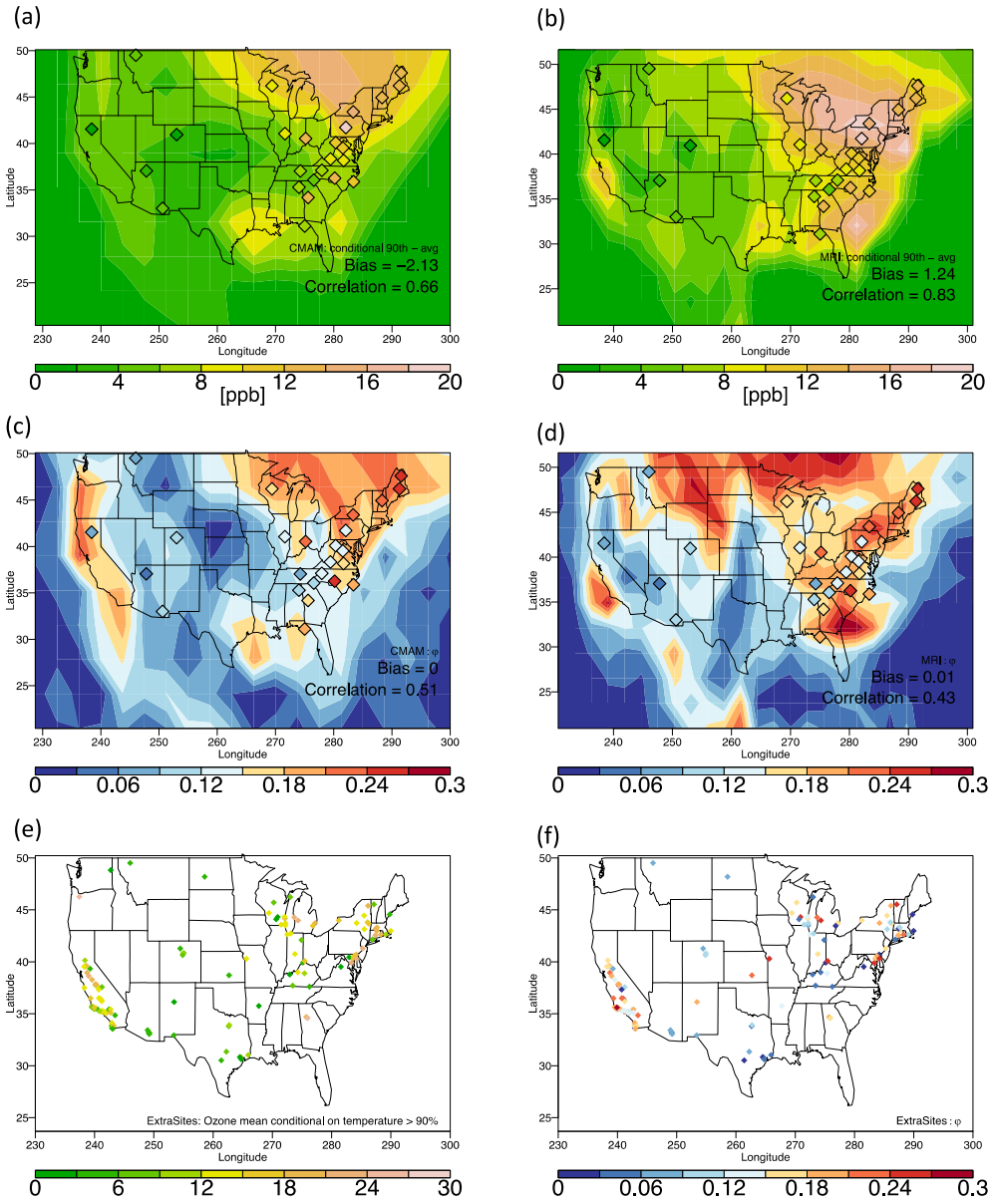

Figure S7 [Rescaled Data] First row: Average MDA8 ozone (ppb) conditioned on daily maximum temperature greater than the 90th percentile minus average MDA8 ozone for JJA 1992-2010 from (a) the CMAM REFC1SD simulation, (b) the MRI REFC1SD simulation. Second row: φ for JJA 1992-2010 from (c) the CMAM REFC1SD simulation, (d) the MRI REFC1SD simulation. CASTNET measurements of each quantity are shown as filled diamonds in the first two rows. In the first two rows we also give: the average bias as the model average minus the CASTNET average for each quantity, and the correlation as the spatial correlation between the model and the CASTNET measurements. Third row: EPA AQS data for JJA 1992-2010 of (e) average MDA8 ozone (ppb) conditioned on daily maximum temperature greater than the 90th percentile minus average MDA8 ozone, (f) φ. The corresponding figures for the CESM1 CAM4-chem are Figure 7 and Figure 9.

Morgenstern, O., Hegglin, M. I., Rozanov, E., O'Connor, F. M., Abraham, N. L., Akiyoshi, H., Archibald, A. T., Bekki, S., Butchart, N., Chipperfield, M. P., Deushi, M., Dhomse, S. S., Garcia, R. R., Hardiman, S. C., Horowitz, L. W., Jöckel, P., Josse, B., Kinnison, D., Lin, M., Mancini, E., Manyin, M. E., Marchand, M., Marécal, V., Michou, M., Oman, L. D., Pitari, G., Plummer, D. A., Revell, L. E., Saint-Martin, D., Schofield, R., Stenke, A., Stone, K., Sudo, K., Tanaka, T. Y., Tilmes, S., Yamashita, Y., Yoshida, K., and Zeng, G.: Review of the global models used within phase 1 of the Chemistry–Climate Model Initiative (CCMI), Geosci. Model Dev., 10, 639-671, https://doi.org/10.5194/gmd-10-639-2017, 2017.